# Half-lives of $^{132}$La and $^{135}$La

E. P. Abel, H. K. Clause, J. Fonslet, R. J. Nickles, and G. W. Severin

# The Half-lives of $^{132}$La and $^{135}$La

E.P. Abel,[1] H.K. Clause,[1] J. Fonslet,[2] R.J. Nickles,[3] and G.W. Severin[1]

[1]*Department of Chemistry and NSCL/FRIB Laboratory,*

*Michigan State University, East Lansing, MI 48824 USA*

[2]*Hevesy Laboratory, Center for Nuclear Technologies,*

*Technical University of Denmark, 4000 Roskilde, Denmark*

[3]*Department of Medical Physics, University of*

*Wisconsin-Madison, Madison WI, 53706 USA*

(Dated: February 14, 2018)

## Abstract

The half-lives of $^{135}$La and $^{132}$La were determined via serial gamma spectroscopy, and the half-life of $^{135}$La was further determined by a high-precision ionization chamber measurement. The results are 18.91(2) hr for $^{135}$La and 4.59(4) hr for $^{132}$La compared to the previously compiled values of 19.5(2) hr and 4.8(2) hr, respectively. These lanthanum isotopes comprise a medically interesting system with positron emitter $^{132}$La and Auger electron emitter $^{135}$La forming a theranostic pair for internal diagnostics and therapeutics. The precise half-lives are necessary for proper evaluation of their value in medicine and for a more representative tabulation of nuclear data.

# I. INTRODUCTION

In medical applications, $^{132}$La and $^{135}$La can be used together as a diagnostic and therapeutic pair, or a "theranostic" pair. Theranostic pairs allow an accurate calculation of dosimetry in internal radionuclide therapy, thereby providing a prediction for the efficacy of treatment (see for example, the theranostic terbium isotopes [1]). However, inaccuracy in half-life values in either isotope will result in a miscalculation of dosimetry and will systematically lower the predictive capability. Clearly, it is important to have accurate and precise nuclear data when performing medical procedures with radionuclides, and this has led to the measurement and re-evaluation of several half-lives over the past few years (for example [2] and [3]).

In the process of investigating this radionuclide pair [5], we discovered that not only are the evaluated half-lives relatively imprecise compared to other nuclear data, but they are also inaccurate. Previously measured half-lives for $^{135}$La are shown in Table 1 where the *Nuclear Data Sheets* (NDS) value is a weighted average of the first and second half-lives listed. These values produce the previously accepted half-life of 19.5(2) hr for $^{135}$La [10]. Similarly, $^{132}$La was also found to have an inaccurate and imprecise half-life. The accepted half-life of 4.8(2) hr for this radionuclide is based on a single value from W.R. Ware and E.O. Wiig in 1960 [11, 12].

The present work uses gamma spectroscopy to elucidate the radionuclide budget and decay curves for $^{132}$La and $^{135}$La in a mixed-species solution. Additionally, the precision of the measured $^{135}$La half-life was improved with an ionization chamber measurement.

# II. MATERIALS AND METHODS

## A. Source Preparation

Two separate radiolanthanum sources were prepared for this experiment by the same procedure with slight variations. The values for the first source, Source 1, are given in the text with the values for the second source, Source 2, appearing in parentheses afterward.

The lanthanum isotopes were created by proton induced reactions on metallic $^{nat}$Ba using a GE-PETtrace cyclotron with nominal incident energy of 16.5 MeV. A 320 mg (640 mg) chunk of barium metal (99.99% dendritic, Sigma Aldrich), was pressed into an aluminum

washer sandwiched between two 50 $\mu$m niobium foils. This was irradiated at 90°incidence with a 10 $\mu$A proton beam for 90 min (70 min). After irradiation, the barium target and niobium foils were removed from the washer and submerged in 5 mL of 3 M nitric acid (Optima, VWR). The barium dissolved, but the niobium remained intact. A 4 mL (5 mL) fraction of the resulting solution was added to 2 mL (3 mL) of 6 M nitric acid to obtain barium nitrate in a 3 M nitric acid solution. This was passed over 98 mg (103 mg) DGA resin (Eichrom) to trap the lanthanum [13]. The resin was washed with 5 mL (10 mL) of 3 N nitric acid, and the lanthanum was eluted with 1 mL of 0.1 M hydrochloric acid (Optima, VWR). Each source elution was split into 200 $\mu$L (500 $\mu$L) fractions.

## B. Gamma Spectroscopy

A fraction of the chemically purified radiolanthanum solution was placed 50 cm (100 cm) from the face of a Canberra C1519 HPGe detector, which was calibrated against $^{133}$Ba, $^{137}$Cs, $^{152}$Eu, $^{241}$Am, and $^{60}$Co standard sources. Counting ensued over the course of the next 90 hr (65 hr), binning data into 10800 s (900 s) live time bins, using an Ortec Aspec 927 ADC and Maestro spectrum software. The ADC deadtime was 32 $\mu$s per analyzed pulse, with initial count rates on the order of $10^3$ analyzed pulses per second. After 10 days elapsed, the sample was counted again to qualitatively identify long-lived impurities.

Due to overlapping demands on laboratory equipment there was an unavoidable stretch

TABLE I. Previous half-life measurements from $^{135}$La decay and the half-life resulting from this work.

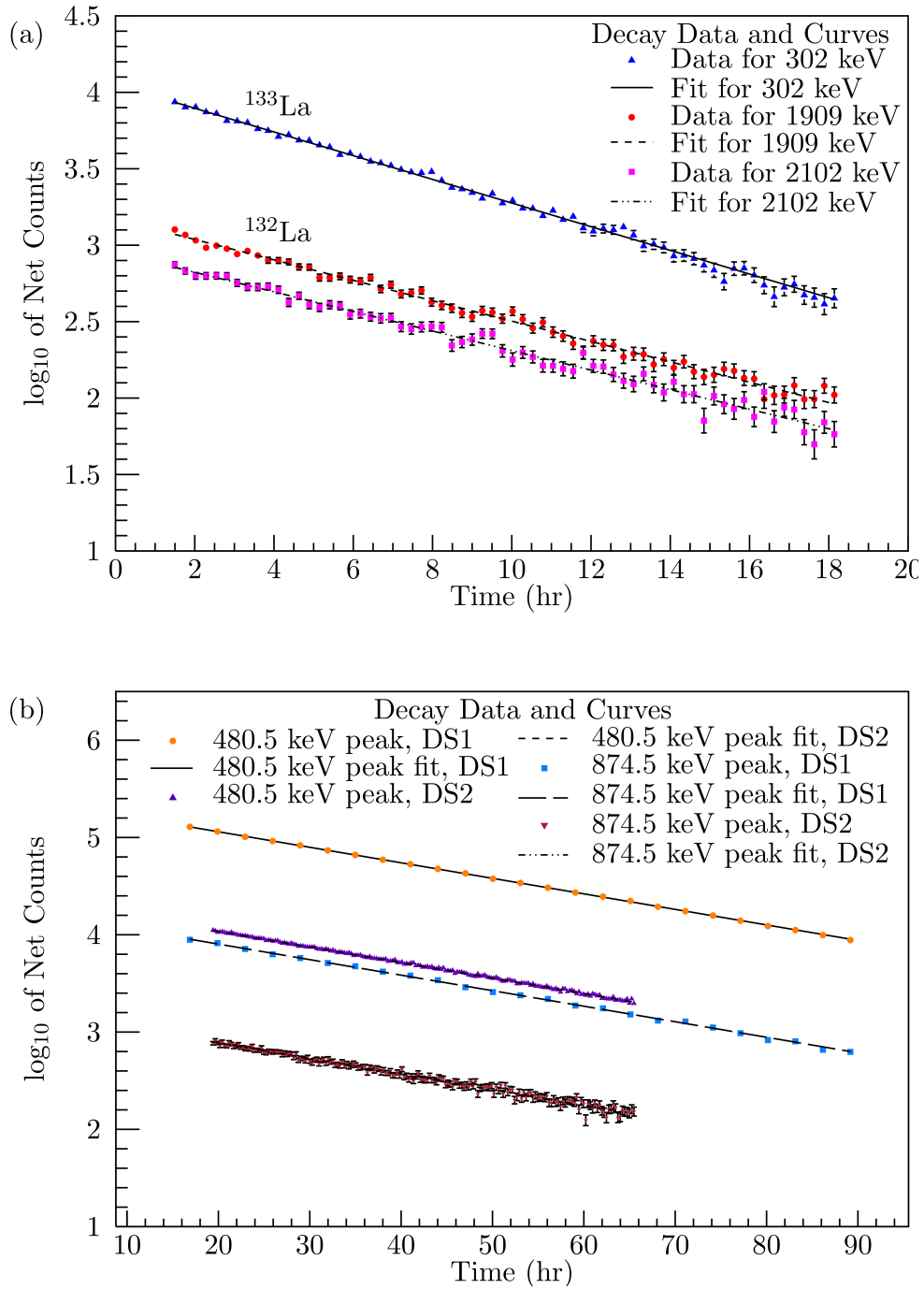| Reference | $t_{1/2}$ (hr) | $\sigma$ (hr) |
|---|---|---|
| Morinobu [4], 1965 | 19.4 | 0.1 |
| Mitchell [6], 1958 | 19.8 | 0.2 |
| Lavrukhina [7], 1960 | 19.7 | – |
| Chubbuck [8], 1948 | 19.5 | – |
| Weimer [9], 1943 | 17.5 | 0.5 |
| NDS value [10] | 19.5 | 0.2 |
| This work, 2017 | 18.91 | 0.02 |

FIG. 1. Decay curves for $^{132}$La, $^{133}$La, and $^{135}$La. (a) Decay curves for $^{132}$La and $^{133}$La, generated from the HPGe data peak-sums at 302, 1909, and 2102 keV from Data Set 2. (b) Decay curves for $^{135}$La generated from the HPGe data peak-sums at 480.5 and 874.5 keV from Data Set 1 (DS1) and Data Set 2 (DS2). The functions resulting from fitting these data points with Equation 2 are plotted as lines for each set of points.

of time during the data collection with Source 2 where $^{72}$As was within the field of view of the detector. Those data were not used in the analysis.

## C.  Ionization Chamber

A fraction of Source 2 was placed in a refitted Capintec CRC CR-2 re-entrant ionization chamber. The chamber had been previously filled with 10 atm pure argon, and was operated at +300V with voltage control and current measurement by a Keithley 6517a ammeter. The current was logged every 10 s with a LabView controlled ADC for ten days without cessation or removal of the source. During the measurement, the current decayed from 150 nA down to 0.03 nA. The ammeter was set to change scale in order to retain precision, and a scale-change occurred at the initiation of the measurement, and once again when the current dropped below 11 nA. The background signal was dependent upon the scale setting, and this required different background correction to be applied to the data. For more information, see Results and Supplemental Materials[14]. To validate the methodology and linearity of the ionization chamber, a $^{64}$Cu source was prepared covering the same range of currents. The $^{64}$Cu source was created by proton bombardment of enriched $^{64}$Ni, and contained small impurities of $^{61}$Cu and $^{61}$Co, which were easily distinguished in the decay curve.

TABLE II. Approximate activities for lanthanum isotopes in Source 2 calculated from the 480.5 keV ($^{135}$La), 302 keV ($^{133}$La), and 1909 keV ($^{132}$La) peaks at the first time point used for finding the respective half-lives via gamma spectroscopy. Time is given as "time after irradiation" to allow comparison between isotopes.

| Isotope | Time after Irradiation (hr) | Activity (MBq) |
| --- | --- | --- |
| $^{135}$La | 19.7 | 45 |
| $^{133}$La | 2.2 | 13 |
| $^{132}$La | 2.2 | 1.5 |

## III. RESULTS

### A. Source Characterization

Gamma spectrum identification of nuclides indicated the presence of $^{131}$La, $^{132}$La, $^{132m}$La, $^{133}$La, $^{135}$La in the earliest measurement, starting 2 hours (55 minutes) after bombardment and 45 minutes (15 minutes) after separation. Undoubtedly, $^{134}$La and $^{136}$La were co-produced, but had decayed below the detection limit at the beginning of sampling. Also, $^{135m}$Ba was co-produced in the beam, but was not present in the sample spectra at any time, reflecting the efficiency of the barium removal. Barium isotopes, $^{131}$Ba and $^{133}$Ba, were qualitatively identified after the counting experiment ended (and the geometry was altered) but their characteristic gamma peaks were not discernible above background in any of the gamma spectra used for analysis. These isotopes formed as daughter products of the lanthanum parents after the initial chemical separation. Within the room there was a background of $^{56}$Co, and the normal natural spectrum from $^{214}$Bi, $^{214}$Pb, and $^{40}$K. As mentioned previously, $^{72}$As was present between hours 18 and 19 during data collection for Source 2 due to other work in the laboratory. No cesium nuclides were identified (as expected due to the low affinity for alkali ions to DGA resin), and the only induced daughter, $^{131}$Cs, was not observed due to the lack of characteristic gamma lines. Also absent was $^{93m}$Mo, which is present in the niobium foil, but was not dissolved into solution or carried through the separation on DGA. The activities of the lanthanum radionuclides at the beginning of the data considered in the determination of the half-lives are given in Table 2. For spectra, see Supplementary Materials[14].

### B. Gamma Spectroscopy Results

For the gamma spectroscopy analysis, data were collected from both Source 1 and 2 to produce Data Set 1 and 2, respectively. Data Set 1 had collection periods of 3 hours and was therefore used only for the determination of the half-life of $^{135}$La. Data Set 2 had much shorter collections periods at 15 minutes each and was used for the half-life measurement for $^{132}$La, $^{133}$La, and $^{135}$La. Characteristic gamma lines were chosen for each of the isotopes: 1909 and 2102 keV for $^{132}$La, 302 keV for $^{133}$La, and 480.5 and 874.5 keV for $^{135}$La. For each of these peaks, a linear baseline correction was calculated by averaging the baseline in

6

surrounding energy bins and was then subtracted from each of the peak sums. To account for the effect of the dead time on the peak sums, the total counts observed, $O(t_1, t_2)$, in each spectrum between the start time, $t_1$, and the end time, $t_2$, were fit using Equation 1:

$$O(t_1, t_2) = \int_{t_1}^{t_2} R(t)dt = \int_{t_1}^{t_2} B + \sum_j \epsilon_j A_j e^{-\lambda_j t} dt, \tag{1}$$

where $R(t)$ is the total observed count rate. This function is described as a constant background event rate, B, and a series of exponential terms for each nuclide, $j$, present in the sample. Each nuclide also has an associated event detection efficiency, $\epsilon_j$, initial activity, $A_j$, and decay constant, $\lambda_j$. This function was approximated as a background and two exponential terms to capture the effect of the dead time on the peak sums. These two exponential terms corresponded to a shorter and a longer lived species but not to any radionuclide in particular. The total observed count rate is then related to the observed peak sums, $S_n(t_1, t_2)$ by Equation 2:

$$S_n(t_1, t_2) = \int_{t_1}^{t_2} (1 - rR(t))\epsilon_n A_i e^{-\lambda_i t} dt, \tag{2}$$

for each peak, $n$, and each radionuclide, $i$. Also, the dead time of 32 $\mu$s per event analyzed is given by $r$ and the detector efficiency and branching ratio for each peak, $n$, is given by $\epsilon_n$. The data for each peak, along with the fitted peak-sum function, are plotted in Figure 1. The half-lives resulting from these fits are given in Table 3.

This method of measuring half-lives was validated by measuring the half-life of $^{133}$La, which has a precise accepted value. This half-life was found to be 3.89(3) hr in this work which agrees well with the accepted value of 3.912(8) hr [15].

## C. Ionization Chamber Results

Ionization chamber current measurements recorded during the period from 3 hours to 9 days after the separation of Source 2 were used to determine the $^{135}$La half-life. Before fitting the data, a subtraction was made to account for the contribution from $^{131}$Ba and $^{131}$Cs that formed as result of $^{131}$La decays during the measurement. Owing to their small quantities in the source, rigorous quantification was not possible. Therefore, the mass 131 correction was performed by assigning a detector response to each nuclide by relating them
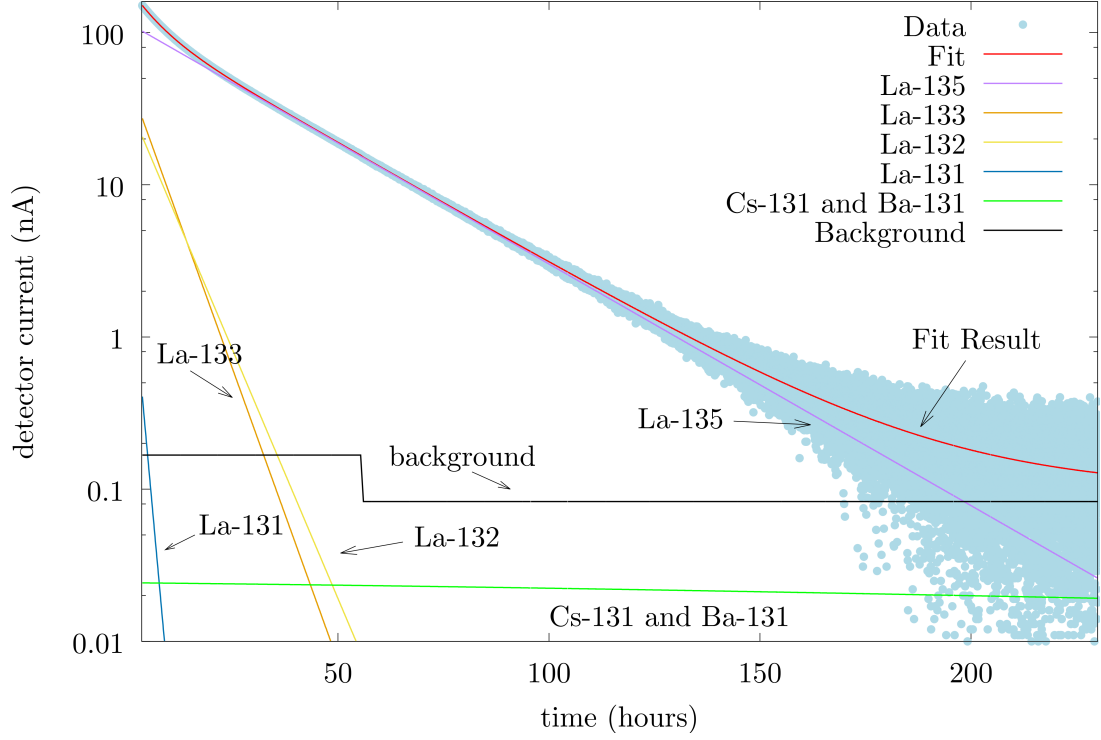
FIG. 2. Plot of current amplitude measurements of the ionization chamber data for $^{135}$La with the resulting fitted function included.

to the detector response for $^{131}$La according to their x-ray and gamma emissions. Using the calculated detector responses with the quantity of $^{131}$La present at the time of chemical separation gave an estimate for the amount of signal in the detector from $^{131}$Ba and $^{131}$Cs at all times, which was subtracted from the entire data set. For reference, the computed $^{131}$Ba

TABLE III. Measured half-lives for $^{135}$La, $^{132}$La, and $^{133}$La from gamma spectroscopy.

| Data Set | Peak Energy (keV) | $t_{1/2}$ (hr) | Average $t_{1/2}$ (hr) |
|---|---|---|---|
| 1 | 480.5 | 18.86(4) | |
| 1 | 874.5 | 18.9(1) | |
| | | | 18.85(3) |
| 2 | 480.5 | 18.85(5) | |
| 2 | 874.5 | 18.8(2) | |
| 2 | 1909 | 4.71(7) | |
| | | | 4.59(4) |
| 2 | 2102 | 4.52(5) | |
| 2 | 302 | 3.89(3) | 3.89(3) |

8

and $^{131}$Cs signal ranged from 0.04 nA to 0.02 nA over the entire data set, where the precision of any individual data point was 0.07 nA. The detector response estimation and the effect on the half-life uncertainty from this correction are treated in detail in the Supplemental Materials[14].

After the correction, the total detector response, $y$, was fit with a multi-exponential function shown in Equation 3, representing contributions to the signal from $^{135}$La, $^{133}$La, $^{132}$La, and $^{131}$La:

$$y = \sum_n A_n e^{-t\lambda_n} + B. \tag{3}$$

This multi-exponential function includes the initial signal, $A_n$, of each nuclide, $n$, at time zero, the respective decay constant of each nuclide, $\lambda_n$, and the time at which the measured current was recorded, $t$. Owing to the scale change on the ammeter, an additional step-function background, $B$, was introduced as a free-fit parameter, with separate values for the time period when the ammeter was on the two different scales. The effect that this additional term has on the precision of the half-life measurement is treated in detail in the Supplemental Materials[14]. In addition to the background component, the signal amplitude, $A_n$, for each nuclide and the decay constant for $^{135}$La were allowed to float. All other half-lives were fixed during the fit using their respective published values– with the exception of $^{132}$La, where the measured half-life of 4.59(4) hr from the HPGe result in Table 3 was used.

In order to weight the data in the fit, the precision of each current measurement was estimated by examining the intrinsic scatter in the data points. This was done by performing a running average across fifty data points at a time, using twenty-five on either side of a single point of interest and taking the absolute value of the difference between the measured value, $y$, and the running average. These values were treated as residuals, and were smoothed by a running root mean square using one-hundred data points at a time. The smoothed residuals, $\Sigma(x)$, were fit with a function that included a statistical term, represented by the square root of a constant, $C_1$, multiplied by the measured current, $x$, and a constant instrumental term, $C_2$, added in quadrature, as shown in Equation 4:

$$\Sigma(x) = \sqrt{C_1 x + C_2^2}. \tag{4}$$

This computed precision, $\Sigma(x)$, was used to weight the data, $y$, for fitting with OriginPro9. The data points and fitting function are shown in Figure 2. The resulting half-life of $^{135}$La was 18.960(2) hr, where the uncertainty only accounts for statistics.

To determine the presence of any systematics resulting from non-linearity in the ionization chamber and ammeter, the methodology was validated using $^{64}$Cu under the same conditions, where $^{61}$Cu and $^{61}$Co were also present. The measured half-life of $^{64}$Cu was 12.6975(5) hr compared to the reference value of 12.701(2) hr [16]. Assuming that the difference between the evaluated half-life and the ionization chamber measurement results from an imprecision in the experimental methodology, the systematic uncertainty assigned to linearity for the measurement was set at 0.28 parts per thousand.

Additionally, the contributions to the precision from the uncertainty in the early background (0.028 hr), the late background (0.013 hr), and the detector response found for $^{131}$Cs and $^{131}$Ba (0.007 hr) were treated as independent and added in quadrature to the linearity uncertainty and the statistical precision. This resulted in a final $^{135}$La half-life value of 18.96(3) hr from the ionization chamber measurement.

### D. Final Results

Through gamma spectroscopy and the ionization chamber measurement, five different half-life measurements were performed for $^{135}$La. These five data points along with the previously accepted half-life are plotted in Figure 3. The values found in this work were averaged using the error of each measurement as respective weights. The final value for the half-life of $^{135}$La was measured to be 18.91(2) hr. As stated above, the half-life of $^{132}$La was found to be 4.59(4) hr, with the precision determined entirely by statistics.

Plots of residuals for the described fits, a description of the uncertainty treatment, and summaries of the measurements according to the prescribed methodology of Pommé are given in the Supplemental Materials [14, 17].

## IV. DISCUSSION

In analyzing the gamma spectroscopy data, careful thought was given to what section of data should be included in the final half-life value. For all of the peaks that were considered,
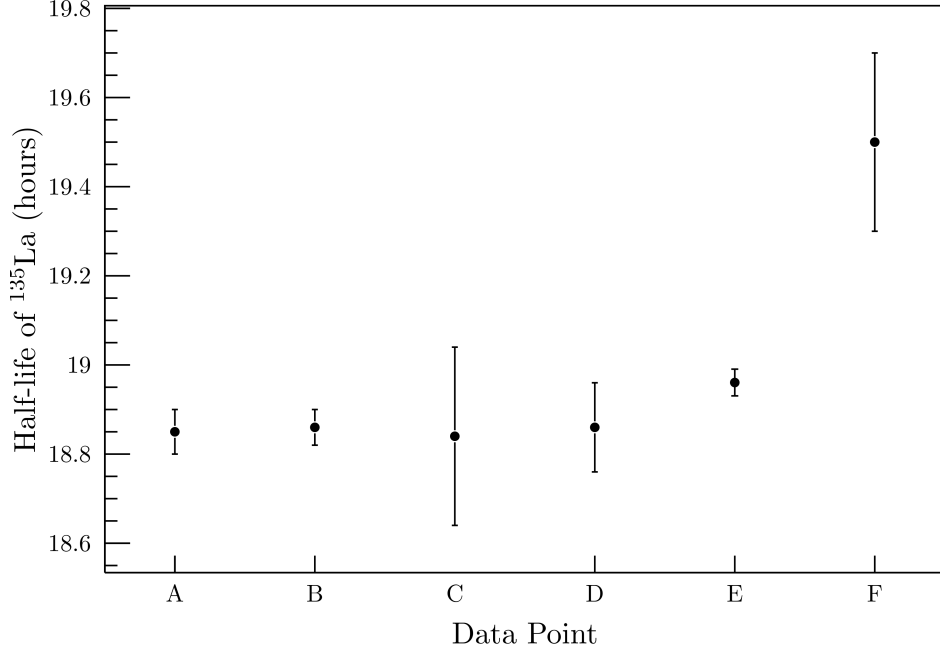
FIG. 3. Plot showing the 5 measurements for the half-life of $^{135}$La in this work and the Nuclear Data Sheet value. Data points A-E are the half-lives measured using the 480.5 keV peak in Data Set 2, the 480.5 keV peak in Data Set 1, the 874.5 keV peak in Data Set 2, the 874.5 keV peak in Data Set 1, and the ionization chamber measurement, respectively. Data point F is the previously accepted value in NDS.

data within the first hour and fifteen minutes was discarded due to a very high count rate in the sample. This count rate would have interfered with fitting the dead time correction and could have introduced many short lived contaminant peaks in the peaks of interest. Of particular importance was the $^{132m}$La contamination which can populate the ground state of $^{132}$La. Excluding the first hour and fifteen minutes of data collected ensured that the contribution to $^{132}$La from $^{132m}$La was less than 0.5% at the start of data analysis for the half-life. Therefore, this possible contamination was found to be irrelevant in the data considered.

For $^{135}$La, data points starting at 19 hours after irradiation for Data Set 1 and 19.7 hours for Data Set 2 were considered in the half-life values. These data were chosen due to contaminant gamma rays in the 480.5 keV and 874.5 keV peaks for $^{135}$La: 479.5 keV from $^{132}$La and 481.5 keV and 874.8 keV from $^{133}$La. Since $^{132}$La and $^{133}$La had few observed counts by hour 18, these contaminating gamma rays, which already have a low intensity,

11

had an insignificant contribution to either peak. In Data Set 1, one single data point for the 480.5 keV peak (from 23 to 26 hours after irradiation) appears to be an outlier, but there is no known cause. The half-life for $^{135}$La was found for the 480.5 keV peak with and without this supposed outlier, resulting in half-lives of 18.85(4) and 18.83(3) hours, respectively. Clearly, this outlier did not have a pronounced effect on the half-life as the two values are consistent with respect to the precision, and as a result, we included the outlier in the fit leading to the value presented in Table 3.

The final time-point used for finding the half-lives of the short-lived lanthanum isotopes was also carefully decided. Since $^{132}$La and $^{133}$La have half-lives on the order of a few hours, only data through 18 hours after the start of the data collection were used in the half-life. At this point, other work in the lab created an increase in the total count rate in the detector, so this was chosen as the cut off for the half-life data for $^{132}$La and $^{133}$La. After this point, very few counts were observed in the peaks for these isotopes showing that this was also a natural stopping point.

## V.   CONCLUSION

Using two different radiolanthanum sources and data from gamma spectroscopy and ionization chamber measurements, the half-lives of $^{132}$La and $^{135}$La were measured. In this work, the half-life of $^{132}$La was found to be 4.59(4) hours and the half-life of $^{135}$La was measured as 18.91(2) hours. As these two lanthanum isotopes are medically relevant, these corrected values will aid in calculating the dose that will result from using these isotopes in medical research. In addition, these corrected values provide more accurate and precise data for the nuclear community to use in future work.

### Acknowledgements

---

[1] C. Müller, M. Bunka, S. Haller et.al, J. Nucl. Med. **55**, 1658 (2014).

[2] S.M. Collins, S. Pommé, S.M. Jerome, K.M. Ferreira, P.H. Regan and A.K. Pearce, Appl. Radiat. Isotop. **104**, 203-211 (2015)

[3] S.M. Collins, A.K. Pearce, K.M. Ferreira, A.J. Fenwick, P.H. Regan and J.D. Keightley,Appl. Radiat. Isotop. **99**, 46-53 (2015)

[4] S.Morinobu, T.Hirose, and K.Hisatake,  Nucl.Phys. **61**, 613 (1965).

[5] J. Fonslet, B. Q. Lee, T.A. Tran, M. Siragusa, M. Jensen, T. Kibédi, A.E. Stuchbery, and G.W. Severin Phys. Med. Biol. **in press** (2017) https://doi.org/10.1088/1361-6560/aa9b44.

[6] A.C.G.Mitchell, C.B.Creager, and C.W.Kocher,  Phys.Rev. **111**, 1343 (1958).

[7] A.K.Lavrukhina, G.M.Kolesov, and Tan Syaoen, Columbia Tech. Transl. **24**, 1117 (1961).

[8] J.B.Chubbuck and I.Perlman,  Phys.Rev. **74**, 982 (1948).

[9] K.E.Weimer, M.L.Pool, and J.D.Kurbatov,  Phys.Rev. **63**, 67 (1943).

[10] B. Singh, A.A. Rodionov, and Y.L. Khazov, Nuclear Data Sheets. **109**, 517 (2008).

[11] Yu. Khazov, A.A. Rodionov, B. Singh, and S. Sakharov, Nuclear Data Sheets. **104**, 497 (2005).

[12] A.R.Ware and E.O.Wiig, Phys. Rev **117**, 191 (1960).

[13] E.P. Horwitz, D. R. McAlister, A.H. Bond, and R.E. Barrans Jr., Solvent Extr. Ion Exc. **23**, 319 (2005).

[14] See Supplemental Material at (URL) for background corrections applied to ionization chamber data, example gamma spectra, a description of how the uncertainty in the ionization chamber was treated, plots of the residuals from all fits described in the paper, and tables of information to satisfy the methodology of Pommé.

[15] Yu. Khazov, A. Rodionov, and F.G. Kondev, Nuclear Data Sheets. **112**, 855 (2011).

[16] B. Singh, Nuclear Data Sheets.**108**, 197 (2007).

[17] S. Pommé, J. Camps, R. Van Ammel, and J. Paepen,J Radioanal Nucl Ch.**276**, 335 (2008).